AKADÉMIAI KIADÓ

UNIVERSITY of DEBRECEN

International Review of Applied Sciences and Engineering

13 (2022) 2, 185–196

DOI:
10.1556/1848.2021.00333
© 2021 The Author(s)

CASE STUDY

Compressive behavior of light–gauge steel tubes filled with concrete containing recycled aggregates

Alaa Sulaiman[1*], Yasser Hunaiti[1], Mu'tasim Abdel-Jaber[1,2] and Ma'en Abdel-Jaber[3]

[1] Civil Engineering Department, Faculty of Engineering, The University of Jordan, Amman, Jordan

[2] Civil Engineering Department, Faculty of Engineering, Al-Ahliyya Amman University, Amman, Jordan

[3] School of Construction Technology and Built Environment, Faculty of Engineering, AlHussein Technical University, Amman, Jordan

Received: June 27, 2021 • Accepted: August 30, 2021
Published online: October 25, 2021

ABSTRACT

The axial capacity of light–gauge steel tube columns filled with concrete including recycled asphalt pavement (RAP) aggregates and recycled concrete aggregates (RCA) was investigated. A total of 51 specimens, including 6 bare steel tubes, 30 composite columns and 15 concrete-only columns were tested under uniaxial load. Fifteen concrete mixes were considered by replacing the weight of natural coarse aggregates (NA) with RCA and RAP at replacement levels of 0, 20, 40, 60, 80, and 100%. In addition, RAP and RCA were combined in the same mixes with replacement levels of (1) 20% RAP and 80% RCA; (2) 40% RAP and 60% RCA; (3) 60% RAP and 40% RCA; and (4) 80% RAP and 20% RCA. Experimental results were analyzed by reporting the ultimate capacities and the patterns of failure. Moreover, the predictions of EUROCODE 4 (EC4) and American Institute of Steel Construction (AISC) codes were checked. ABAQUS software was used to perform a finite element analysis (FEA) of the tested composite specimens. The results showed that using recycled aggregates decreased the carrying capacity of columns. Carrying capacity of light–gauge steel tubes filled with concrete including different combinations of RCA, NA and RAP aggregates can be conservatively predicted by the AISC and EC4 recommendations. Results of FEA showed a good agreement with the experimental results.

KEYWORDS

axial load, composite columns, recycled asphalt pavement aggregates, recycled concrete aggregates, steel tube

1. INTRODUCTION

The concrete-filled steel tube (CFST) columns are extensively used in structures subjected to large, applied moments, especially in high seismic risk zones. CFST columns are characterized by their high capacity and ductility. They have larger energy absorption compared to conventional steel and reinforced concrete columns. The enhancement in the structural characteristics of CFST columns is due to the composite action between the concrete core and the steel tube. The concrete core delays the bending and local buckling of the steel tube, while confinement of concrete through the steel tube enhances the strength and ductility of the concrete core. On the other hand, the steel tube works as column formwork in casting concrete and acts as longitudinal and transverse reinforcement, and thus it reduces the construction cost [1–4].

Extensive research has been conducted to study the behavior of CFST using conventional materials for concrete and steel under uniaxial load [1–4]. The research showed that concrete plays an important role in the capacity of CFST columns. Some researchers have tried to use

*Corresponding author.
E-mail: sulaiman_alaa@yahoo.com

AKJournals

Brought to you by University of Debrecen | Unauthenticated | Downloaded 06/17/22 01:51 PM UTC

new types of concrete other than conventional concrete to construct composite columns such as foamed and lightweight aggregates concrete [5, 6]. Recently, most of the research related to the study of improving properties of the concrete mix has been directed to investigate the effect of using recycled aggregates (RA) as an alternative to natural aggregates (NA) in the concrete mixture. The most used sources of RA are construction waste (crushed concrete, bricks...) and bituminous materials from roads maintenance.

Many researchers investigated whether recycled concrete aggregates (RCA) produced by crushing the construction waste could be used as a replacement of NA in concrete mixtures. The studies showed that using RCA reduces the mechanical properties of concrete. This reduction depends on the quantity of RCA, and the source of original concrete used to produce the RCA [7, 8]. Studies on the possibility of using recycled asphalt pavement (RAP) aggregates obtained by crashing the waste of roads maintenance in concrete mixtures have recently begun [9–13]. The studies showed that using RAP aggregates as an alternative to natural coarse aggregates in original concrete reduces the mechanical properties of concrete [9, 10]. But using RCA and RAP aggregates in the previous concrete improved the compressive, flexural, and splitting tensile strengths of the previous concrete [11]. Some research was conducted to study the possibility of improving the mechanical properties of concrete containing RAP aggregates by using different enhancing materials such as silica fume and class C fly ash (CFA). Using silica fume enhances the mechanical properties of concrete containing RAP aggregates, where the optimum content of silica fume was found to be 10% [12] while using CFA decreased compressive strength and indirect tensile strength of concrete significantly with the increase of RAP aggregates content [13].

The effect of using RA on the behavior of structural elements has been extensively investigated with RCA [14–17] while using RAP aggregates is limited in reinforced concrete elements and composite beams [18, 19]. In general, the behavior of structural elements including RA is similar to structural elements including normal aggregate, but there is a reduction in ultimate strength capacities.

Based on a review of the available literature, there is a lack of information about the validity of using RAP aggregates in the construction of CFST columns. Therefore, this research investigated the behavior of light–gauge steel tubes (LGST) columns filled with concrete including RCA and RAP aggregates. The concrete mixes were made by replacing NA with RCA and RAP with different replacement ratios. All columns were tested under uniaxial loading. The compressive strength of concrete was recorded, and the test results of RAP and RCA columns were compared with specimens containing only NA. The experimental capacities of the columns were compared with theoretical values calculated according to the American Institute of Steel Construction (AISC) [20] and the Eurocode 4 (EC4) [21]. In addition, a finite element analysis (FEA) was performed using ABAQUS software, and the results were compared with the experimental ones.

2. MATERIALS AND METHODS

2.1. Raw materials

2.1.1. Light–gauge steel tubes. Galvanized light–gauge steel sheets with 2 and 2.4 mm thickness (t) were used to fabricate the square steel tubes with 100 mm depth (D) and 1 m length. Steel thickness was chosen based on the availability of steel in the local market. Steel sheets were cut and formed to produce two pieces with shapes and dimensions shown in Fig. 1(a). The two pieces were welded using an Exx70 welding type with 3-mm thickness to construct the steel tubes as shown in Fig. 1(b). The tensile test of steel was performed according to ASTM A 37 [22] using two specimens for each thickness. The average values of the yield strength (F_y) and the tensile strength (F_u) for steel are shown in Table 1.

2.1.2. Aggregate and cement. NA, RCA, and RAP aggregates are the types of coarse aggregates used in producing the concrete mixes. RCA and RAP aggregates were obtained by crushing concrete cubes and road maintenance wastes, respectively. Concrete cubes were collected from different sites without knowing their compressive strength. NA was obtained from Al-Manaseer crushers located in Al-Karama City, West of Jordan. Particle aggregates sizes for the three types of aggregates range from 20 to 4.75 mm. Locally produced Silica-based sand and Portland-Pozzolana cement CEM II/A-P42.5N were used for all concrete mixes. The Portland-Pozzolana cement was produced according to Jordanian (JS) and European (EN) standards. The physical and chemical properties of cement are summarized in Tables 2 and 3 respectively.

Sieve analysis for the three types of coarse aggregates was made according to ASTM C 136 [23]. Figure 2 shows the coarse aggregates grading chart for the three types with limits specified in ASTM C 33 for 25 mm (1 in.) coarse aggregates [23].

The coarse aggregates properties were determined according to ASTM C 127 [23] and ASTM C29/C29M [23] and shown in Table 4. It can be seen that RA has less specific gravity and bulk density than the NA. According to water absorption, the RCA has the highest value due to the remained mortar layer that coats this type of aggregates, followed by RAP then NA. In some cases, RAP aggregates have the lowest absorption depends on the amount of asphalt that covers the aggregates and prevents them from absorbing water.

2.2. Experimental program

2.2.1. Concrete mix proportions. Fifteen concrete mixes were produced in the structural engineering laboratory by

Brought to you by University of Debrecen | Unauthenticated | Downloaded 06/17/22 01:51 PM UTC

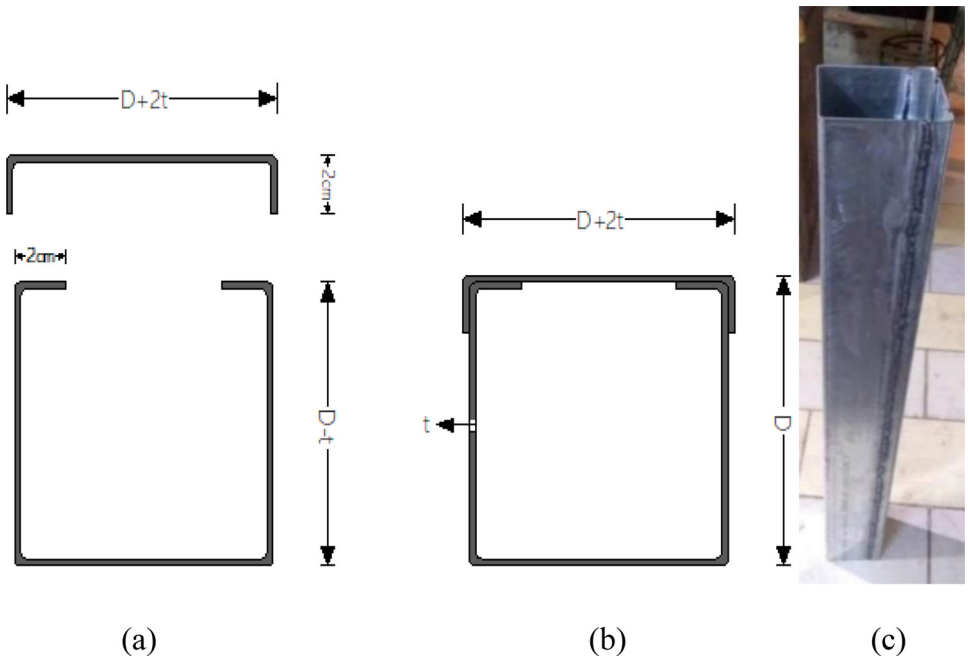

Fig. 1. Cross section details; (a) dimension of steel pieces; (b) cross-section of steel tube; (c) steel tube

Table 1. Light–gauge steel properties

Specimens		Yield strength (MPa)	F_y(MPa)	Tensile strength	F_u(MPa)	Elongation (%)
t = 2 mm	1	221	220	357.2	355.3	12.90
	2	219		353.4		12.50
t = 2.4 mm	1	285	280	350	350	14.90
	2	275		350		14.90

Table 2. Cement physical properties

Physical property	Unit	Result	Testing method	Specification
Fineness by (Blaine)	$cm^2\ g^{-1}$	4,000.0	EN 196-6:1992	
Finene	%	2.5	EN 196-6:1992	
ss by (Residue)-45μm				
Initial setting time	Min	160	JS 1470-3/05 EN 196-3:2005	≤60.0
Finial setting time	Min	225	JS 1470-3/05 EN 196-3:2005	
w/c	%	29.6	JS 1470-3/05 EN 196-3:2005	
Soundness	Mm		JS 1470-3/05 EN 196-3:2005	≤10.0
2 days compressive strength	MPa	24.0	JS 1470-3/05 EN 196-1:2005	≥10.0
28 days compressive strength	MPa	49.0	JS 1470-3/05 EN 196-:12005	≥42.5 ≤ 62.5

replacing NA with RCA and RAP aggregates with replacement levels of (0, 20, 40, 60, 80, and 100%). In addition, NA was totally replaced by a combination of RAP aggregates and RCA using replacement levels of (20, 40, 60 and 80%). All these replacements were carried out by the weight of the coarse aggregates. NA-100 mix was designed to achieve a compressive cube strength of 30 MPa at 28 days. Table 5 shows the mix proportions and the slump test results for all concrete mixes. Water absorption amount for coarse aggregates was added to the mixes to maintain the amount of free water. Concrete mixes including RCA recorded the highest slump test results due to its high-water absorption. Six cubes with 150 mm depth were cast from each mix to determine the actual compressive strength in which all cubes were cured in water until the day of testing.

2.2.2. Test specimens. Fifty-one columns were tested in this study. The columns were arranged in three sets, the first set contained six steel tubes: three tubes from each steel thickness. The second set contained fifteen composite columns from each steel thickness filled with the concrete mixes mentioned in Table 5. Finally, the third set contained fifteen concrete only square columns of 100 mm side and 1 m length. All columns were cast and left without curing in the prevailing weather conditions until the day of testing.

Brought to you by University of Debrecen | Unauthenticated | Downloaded 06/17/22 01:51 PM UTC

Table 3. Cement chemical properties

Chemical composition	Content
SiO_2	24.0 ± 0.5
Al_2O_3	6.5 ± 0.5
Fe_2O_3	6.5 ± 0.5
CaO	52.5 ± 1.0
MgO	3.2 ± 0.5
SO_3	2.60 ± 0.2
K_2O	0.8 ± 0.1
Na_2O	0.95 ± 0.1

Table 4. Coarse aggregates properties

Property	NA	RCA	RAP aggregates
Apparent specific gravity	2.71	2.65	2.32
Bulk dry specific gravity (OD)	2.63	2.24	2.20
Bulk specific gravity saturated surface dry (SSD)	2.66	2.4	2.25
Water absorption (%)	1.23	6.92	2.42
Bulk density (unit weight) (kg m^{-3})	1,670	1,371	1,316

2.2.3. Test setup. All columns were tested under an increasing axial load after 28 days of age. The test was performed using a 700 kN capacity MFL Prüf-systeme, Universal Testing Machine (Fig. 3(a)) at The University of Jordan laboratories.

2.3. Theoretical capacity

Design codes evaluation of the carrying capacity of CFST columns is based upon the concrete and steel contributions to the resistance of the column. In this study, two codes were used to evaluate the carrying capacity of the CFST column, which are the American Institute of Steel Construction (AISC) [20] code and the EUROCODE 4 (EC4) [21]. Nominal axial load (P_n) for bare steel tubes was calculated according to the American Iron and Steel Institute (AISI) [24]. The ultimate capacity (P_{un}) of concrete only column was calculated according to American Concrete Institute ACI 318-14 [25]. The average cubes strength at 28 days of age was converted to concrete cylinder strength (f'_c) by multiplying its value by 0.84 [26]. The modulus of elasticity of steel (E_s) was assumed to be 200 MPa, while the modulus of elasticity of concrete (E_c) was calculated according to equations in AISC [20] and EC4 [21] codes.

2.4. Finite element analysis

Finite element analysis (FEA) was conducted to calculate the capacity of composite columns using the finite analysis program ABAQUS. The model was calibrated to predict the closest capacity of the composite columns, and the final model is described in this paper.

2.4.1. Part, meshing and assembly. This model contains two main parts, which are the steel tube and the concrete core meshed with an element size of 30 mm. The body of the composite column was assembled by placing the concrete core part inside the steel tube part. Figure 4(a) shows the body of composite column with meshing.

2.4.2. Material definition. Steel was defined as an elastic-plastic material with an assumed Poisson's ratio of 0.3. While for concrete, the mechanical elastic behavior was defined with an assumed Poisson's ratio of 0.2. Young's modulus was determined according to Eq. (1). The plastic

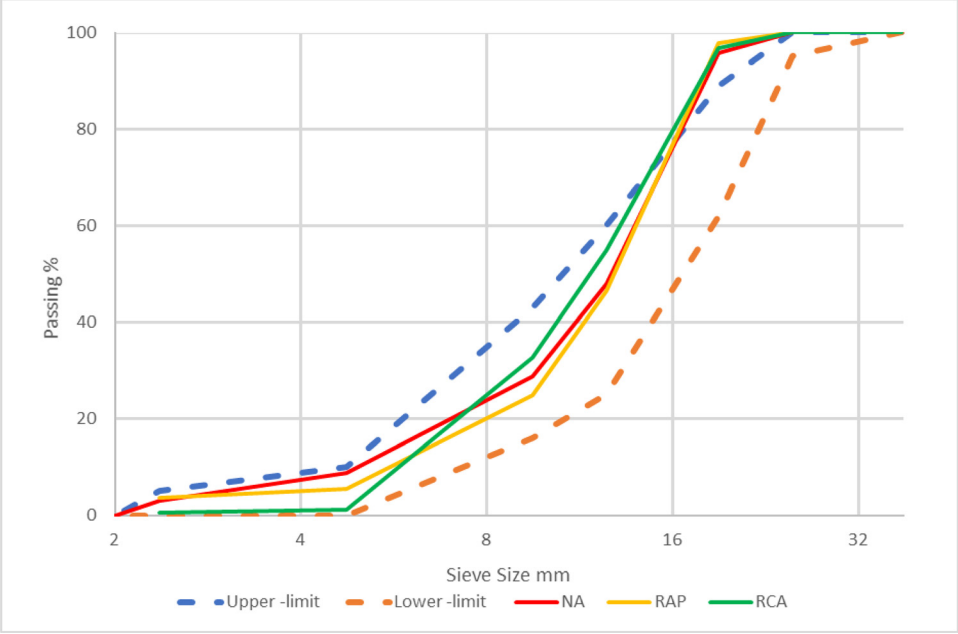

Fig. 2. Aggregates sieve analysis

Brought to you by University of Debrecen | Unauthenticated | Downloaded 06/17/22 01:51 PM UTC

Table 5. Details of mix proportions

Mix type	NA (kg m^{-3})	RAP (kg m^{-3})	RCA (kg m^{-3})	Unit weight (kg m^{-3})	Slump test results (mm)
NA-100	1,145	–	–	2,500	70
RAP-20 & NA-80	916	229	–	2,383	75
RAP-40 & NA-60	687	458	–	2,324	77
RAP-60 & NA-40	458	687	–	2,314	83
RAP-80 & NA-20	229	916	–	2,297	85
RAP-100	–	1,145	–	2,226	105
RCA-20 & NA-80	916	–	229	2,382	85
RCA-40 & NA-60	687	–	458	2,323	105
RCA-60 & NA-40	458	–	687	2,311	112
RCA-80 & NA-20	229	–	916	2,331	135
RCA-100	–	–	1,145	2,248	150
RAP-80 & RCA-20	–	916	229	2,242	110
RAP-40 & RCA-60	–	687	458	2,275	124
RAP-40 & RCA-60	–	458	687	2,266	135
RAP-20 & RCA-80	–	229	916	2,279	145

For all concrete mixes, Cement = 375 kg m^{-3}, Free water = 180 kg m^{-3}, Sand = 638 kg m^{-3}.

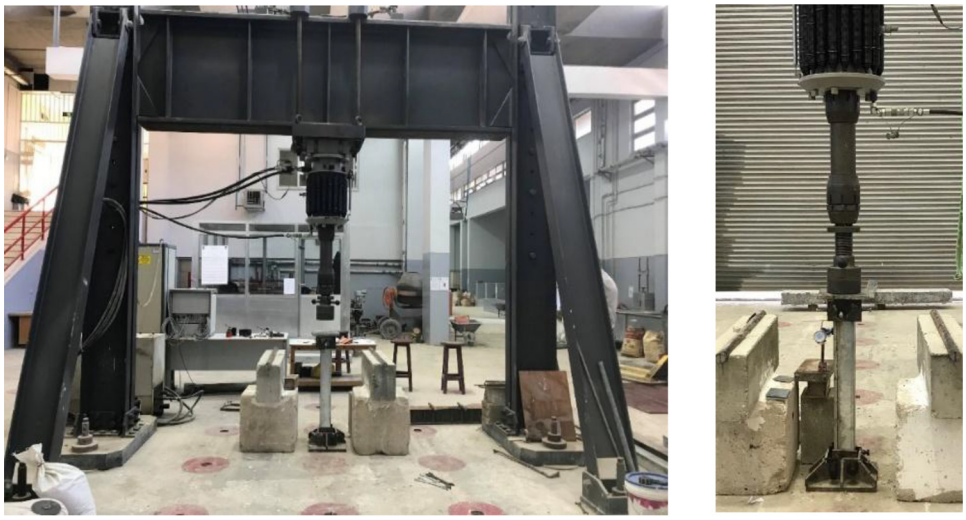

(a) (b)

Fig. 3. (a) Compressive testing machine and (b) Test setup

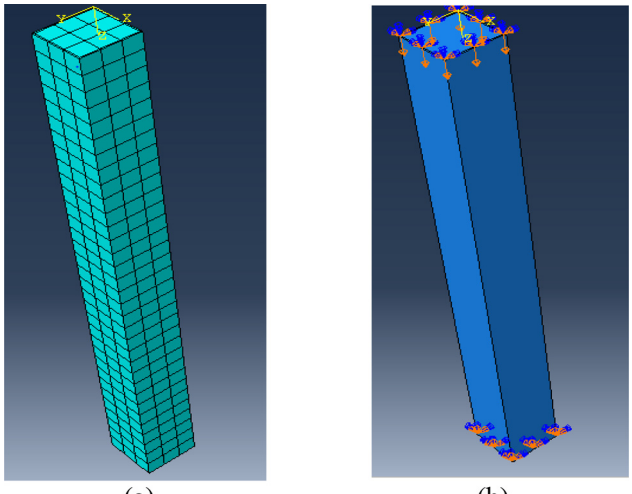

(a) (b)

Fig. 4. (a) Meshing (b) boundary condition

behavior was defined under concrete damage plasticity with parameters mentioned in Table 6.

$$E_c = 4700\sqrt{f_c'} \quad (1)$$

The compressive and tensile stress-strain relationships of concrete were defined based on Tsai's equation for unconfined concrete [27].

2.4.3. Interaction. Interactions must be created between the entire model parts to allow them to act as a unit when any loads or boundary conditions are applied. Surface to

Table 6. Plasticity parameters

Dilation angle	Eccentricity	F_{b0}/F_{c0}	K	Viscosity parameter
37°	0.1	1.16	0.667	0.01

Brought to you by University of Debrecen | Unauthenticated | Downloaded 06/17/22 01:51 PM UTC

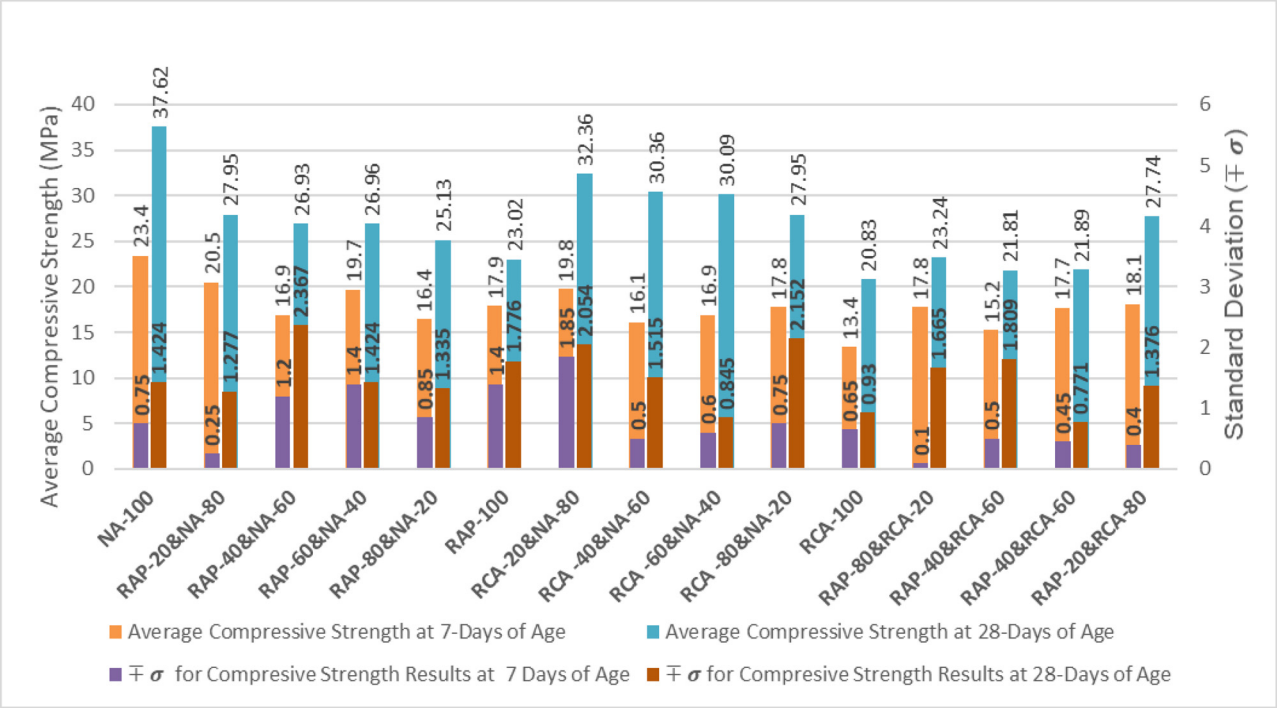

Fig. 5. Average compressive cubes strength and standard deviation ($\mp \sigma$) for compressive cubes strength results

surface interaction has been implemented between the inner surfaces of the steel tube and the outer surfaces of the concrete core with 0.3 friction coefficient and hard contact property.

2.4.4. Boundary condition. The boundary condition for the bottom end of the composite column was chosen as fixed support. The top end was modeled by restraining all the translational and rotational degrees of freedom, except the translational degree of freedom in the axial direction (Fig. 4(b)). The dynamic explicit step was defined in order to perform FEA. The axial deflection was applied to the column, until failure occurred, to simulate the actual test, and the failure loads were obtained and compared with the experimental results.

(a) (b)

Fig. 6. Failure modes; (a) bare steel tubes; (b) concrete only columns

Brought to you by University of Debrecen | Unauthenticated | Downloaded 06/17/22 01:51 PM UTC

3. RESULTS AND DISCUSSION

3.1. Compressive strength of concrete

The compressive strength of each concrete mix was determined by testing six 150 mm cubes. Two cubes were examined at the age of 7 days; other cubes were tested at the age of 28 days. Average compressive strength and standard deviation ($\mp \sigma$) are shown in Fig. 5. It can be seen that the compressive strength of concrete is reduced by using RA. This reduction depends on the source and amount of recycled aggregates used. Increasing the amount of RA reduces the compressive strength. At 28 days of age, RCA & NA combination provided the highest compressive strength except for RCA-100. the maximum compressive strength obtained for RCA cubes is about 32 MPa for RCA-20 & NA-80. For RAP aggregates, the maximum compressive strength was found to be almost 28 MPa for RAP-20 & NA-100. Completely replacing the NA with the recycled aggregates leads to a high reduction in the compressive strength.

3.2. General behavior and failure modes

Failure pattern of bare steel tubes and concrete only columns are shown in Fig. 6. The outward and inward deformation occurred in bare steel tubes at both ends, while concrete-only columns failed by crushing the top of columns.

All composite columns failed by crushing concrete cores. The outward deformation (local buckling) appeared in the steel section for specimens including NA and RAP aggregates, while local buckling did not appear in specimens including RCA and a combination of RCA & RAP aggregates. Figures 7 and 8 shown the failure modes of composite columns.

Fig. 7. Failure modes of composite specimens; (a) NA-100; (b) RAP & NA combinations; (c) local buckling of different specimens

Brought to you by University of Debrecen | Unauthenticated | Downloaded 06/17/22 01:51 PM UTC

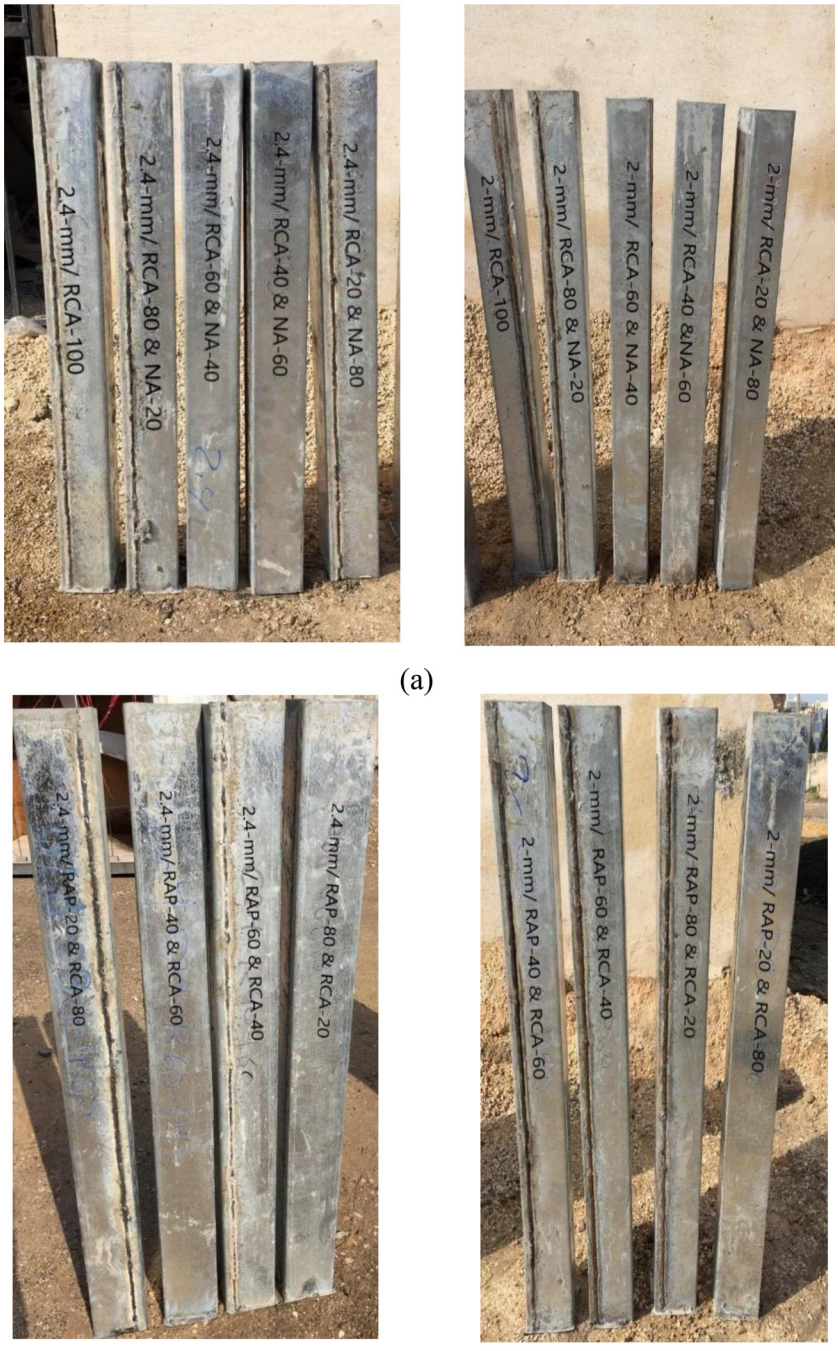

Fig. 8. Failure modes of composite specimens; (a) (RCA & NA) combinations; (b) (RAP & RCA) combinations

3.3. Ultimate load test

Test results of composite and concrete-only columns are given in Table 7. Results revealed that the axial capacity of composite and concrete only columns decreased with the increase of the amount of RCA and RAP aggregates in concrete mixes, this outcome agrees with previous research [14–19]. Composite specimens of RAP-60 & NA-40 and RCA-80 & NA-20 mixes, in addition to concrete-only specimens with RCA-80 & NA-20 mix and composite specimens with 2.4 mm steel thickness and including RAP-40 & RCA-60 mix were discarded from the discussion because their capacity did not match the capacity pattern of other specimens.

According to the results of composite specimens with RAP & NA combination, composite specimens of RAP-80 & NA-20 concrete mix recorded the lowest capacity with a reduction percent of 14 and 18% for 2 and 2.4 mm steel thickness, respectively. The highest capacity was recorded for RAP-20 & NA-80 concrete, with values approximately

Brought to you by University of Debrecen | Unauthenticated | Downloaded 06/17/22 01:51 PM UTC

Table 7. Test results of composite and concrete-only columns

Concrete mix type	Experimental capacity(P_{exp}) (kN)		
	Composite columns		Concrete only columns
	2 mm	2.4 mm	
NA-100	443.60	554.30	305.47
RAP-20 & NA-80	447.27	559.47	245.90
RAP-40 & NA-60	439.27	490.67	238.12
RAP-60 & NA-40	539.47	510.27	227.87
RAP-80 & NA-20	369.27	420.07	183.07
RAP-100	380.50	451.97	158.57
RCA-20 & NA-80	434.17	545.37	250.57
RCA-40 & NA-60	423.17	485.87	269.87
RCA-60 & NA-40	414.07	471.77	238.67
RCA-80 & NA-20	461.07	329.27	254.87
RCA-100	352.27	461.77	190.67
RAP-80 & RCA-20	376.77	477.37	196.27
RAP-60 & RCA-40	354.57	467.97	179.27
RAP-40 & RCA-60	347.47	330.27	182.77
RAP-20 & RCA-80	389.37	482.17	204.14

the same as the composite specimens with NA-100. Reduction percent was recorded as 1 and 11% for 40% RAP composite specimens with 2 and 2.4 mm steel respectively and 14 and 18% for 100% RAP composite specimens with 2 and 2.4 mm steel thickness, respectively. The reduction in capacities of RAP specimens is due to weak bending between RAP aggregates coated with asphalt and concrete mix [18].

The capacity reduction of RCA & NA composite specimens relative to composite specimens including NA-100 was recorded as 2, 5, 7, and 21% for specimens with 2 mm steel thickness including 20, 40, 60 and 100% of RCA respectively, and as 2, 12, 15 and 17% for specimens with 2.4 mm steel thickness and including 20, 40, 60 and 100% of RCA respectively. The highest capacity recorded was for RCA-20 and NA-80 concrete. The capacity decreased with the increase of the RCA amount, this agrees with the conclusions of the research made by Yang and Han [14].

For composite specimens including RAP & RCA combination, the reduction was recorded as 15, 20, 21 and 12% for specimens with 2 mm steel thickness, including RAP-80 & RCA-20, RAP-60 & RCA-40, RAP-40 & RCA-60, and RAP-20 & RCA-80 mixes, respectively, while it was recorded as 14, 16 and 13% for specimens with 2.4 mm steel thickness including RAP-80 & RCA-20, RAP-60 & RCA-40, and RAP-20 & RCA-80 mixes respectively.

For concrete only columns, RCA & NA specimens recorded the lowest reduction in capacity compared with results of RAP & NA specimens and RAP & RCA specimens. Capacity Reductions were 20–48%, 12–38% and 33–41% for groups RAP & NA, RCA & NA, and RAP & RCA respectively.

The composite specimens with RAP gave slightly higher axial loads than those for the RCA composite column specimens at the same NA replacement levels. This might be attributed to the confinement of concrete made using RAP aggregates, as the effect of confinement by the steel tube can be greater compared with the concrete made with RCA aggregates; thus, showed better enhancement that compensated the difference in the compressive strength.

Table 8 shows the test results of bare steel tubes. The average capacity for bare steel tubes with 2 mm thickness was calculated using the results of all specimens. For 2.4 mm steel, the specimen with 208 kN capacity was not within the range of standard deviation, thus it was discarded.

It can be seen that concrete including RA enhances the capacity of steel section in composite columns. The contribution of concrete to the capacity of composite columns with 2 mm was recorded as 56–64% for RAP & NA combination, 54–62% for RCA & NA combination and 53–58% for RAP & RCA combination. For specimens with 2.4 mm, the contribution of concrete was recorded as 37–52%, 43–51% and 43–45% for RAP & NA, RCA & NA, and RAP & RCA combinations respectively.

The results of this study indicate that RAC and RAP are feasible to be used in concrete filled LGST columns as a replacement of NA with low replacement levels, which did not introduce a high reduction in the capacity. This agrees well with the conclusion of the previous literature done by Yang and Han (2006) [14, 17] and El-Nimri et al. (2020) [19].

3.4. Theoretical capacity

The carrying capacities of CFST columns were evaluated by using AISC and EC4 codes are shown in Table 9. Comparing the theoretically predicted values with the experimental results shows that AISC and EC4 methods are conservative for predicting the ultimate capacity of the composite specimens. AISC method gives an ultimate capacity about 19% lower than the experimental results. The ultimate capacity predicted by EC4 is in close agreement with the experimental results for all composite columns except specimens with 2.4 mm steel thickness including RCA-40 & NA-60, RCA-60 & NA-40, and PAP-80 & NA-20 mixes. The predicted capacities of these specimens were about 5, 7, and 13% larger than the experimental results, respectively. For specimens with 2 mm thickness including NA-100 mix and specimens with 2.4 mm thickness including RAP-100 and RAP-20 & RCA-80 mixes, the calculated capacity according to EC 4 was only 2% larger than the experimental results, which lies within an acceptable range of overestimation [1].

Tables 10 and 11 show the nominal axial load (P_n) for bare steel tubes and the ultimate compressive capacity (P_{un})

Table 8. Test results of bare steel tubes

Thickness (mm)	Experimental capacity (P_{exp}) (kN)	Standard deviation ($\mp \sigma$)	Average capacity (kN)
2	173.07	7.42	163
	155.50		
	160.27		
2.4	277.47	35.24	265.17
	207.97		
	252.87		

Brought to you by University of Debrecen | Unauthenticated | Downloaded 06/17/22 01:51 PM UTC

Table 9. Ratio of experimental and theoretical axial loads for AISC and EC 4 code

Concrete mix type	AISC				EC4			
	2 mm		2.4 mm		2 mm		2.4 mm	
	$\phi_c P_n$(kN)	$P_{exp}/\phi_c P_n$	$\phi_c P_n$(kN)	$P_{exp}/\phi_c P_n$	N_{Rd}(kN)	P_{exp}/N_{Rd}	N_{Rd}(kN)	P_{exp}/N_{Rd}
NA-100	359.30	1.23	439.50	1.26	451.50	0.98	554.10	1
RAP-20 & NA-80	311.80	1.43	393.20	1.42	388.50	1.15	492.20	1.14
RAP-40 & NA-60	306.70	1.43	388.30	1.26	381.80	1.15	485.60	1.01
RAP-60 & NA-40	–	–	–	–	–	–	–	–
RAP-80 & NA-20	297.70	1.24	379.50	1.11	370.00	1	474.00	0.89
RAP-100	287.30	1.32	369.40	1.22	356.40	1.06	460.60	0.98
RCA-20 & NA-80	333.50	1.30	414.40	1.32	417.20	1.04	520.30	1.05
RCA-40 & NA-60	323.80	1.31	405.00	1.20	404.40	1.05	507.80	0.96
RCA-60 & NA-40	322.30	1.28	403.40	1.17	402.30	1.03	505.70	0.93
RCA-80 & NA-20	–	–	–	–	–	–	–	–
RCA-100	276.20	1.26	358.60	1.29	341.90	1.03	446.40	1.03
RAP-80 & RCA-20	288.30	1.29	370.30	1.30	357.60	1.05	461.90	1.03
RAP-60 & RCA-40	281.10	1.26	363.40	1.30	348.30	1.02	452.70	1.03
RAP-40 & RCA-60	281.50	1.23	–	–	348.90	0.99	–	–
RAP-20 & RCA-80	310.70	1.25	392.10	1.23	387.00	1.00	490.70	0.98
Mean Value		1.30		1.26		1.044		1.003
Standard Deviation		0.064		0.077		0.0516		0.0607
Coefficient of Variation		0.049		0.061		0.049		0.0605

Table 10. P_n of bare steel tube

Thickness (mm)	P_n (kN)	Average capacity/P_n
2	199.50	0.82
2.4	300.40	0.88

Table 11. P_{un} of concrete only column

Concrete mix type	P_{un} (kN)	P_{exp}/P_{un}
NA-100	268.60	1.14
RAP-20 & NA-80	199.60	1.23
RAP-40 & NA-60	192.30	1.24
RAP-60 & NA-40	192.50	1.18
RAP-80 & NA-20	179.50	1.02
RAP-100	164.40	0.96
RCA-20 & NA-80	231.10	1.08
RCA-40 & NA-60	217.10	1.24
RCA-60 & NA-40	214.80	1.10
RCA-80 & NA-20	–	–
RCA-100	148.70	1.28
RAP-80 & RCA-20	165.90	1.18
RAP-60 & RCA-40	155.70	1.15
RAP-40 & RCA-60	156.30	1.17
RAP-20 & RCA-80	198.10	1.03

of concrete only columns. The nominal axial load (P_n) for bare steel tubes is higher than the average of experimental capacities, which means that specimens have failed before they reach local buckling. For concrete only columns, P_{exp} is greater than P_{un} except for the specimen with RAP-100.

3.5. FEA results

Table 12 compares the experimental capacity (P_{exp}) for composite columns with results of finite element analysis (P_{FE}). The maximum axial load obtained from finite element model showed a close agreement with the experimental results, except NA-100 specimen with 2 mm steel thickness and RCA-40 & NA-60, RCA-60 & NA-40, and PAP-80 & NA-20 specimens with 2.4 mm steel thickness, which give about 4–13% higher than experimental results.

Table 12. Comparison between the P_{exp} of composite specimens and P_{FE}

Concrete mix type	2 mm		2.4 mm	
	P_{FE}	P_{exp}/P_{FE}	P_{FE}	P_{exp}/P_{FE}
NA-100	463.27	0.96	556.18	0.99
RAP-20 & NA-80	395.37	1.13	489.55	1.14
RAP-40 & NA-60	388.82	1.13	482.48	1.017
RAP-60 & NA-40	–	–	–	–
RAP-80 & NA-20	375.85	0.98	477.06	0.88
RAP-100	360.88	1.05	455.34	0.99
RCA-20 & NA-80	427.12	1.02	518.95	1.05
RCA-40 & NA-60	413.28	1.02	507.07	0.96
RCA-60 & NA-40	410.37	1.01	502.02	0.94
RCA-80 & NA-20	–	–	–	–
RCA-100	344.70	1.02	439.24	1.05
RAP-80 & RCA-20	362.19	1.03	452.07	1.06
RAP-60 & RCA-40	352.30	1.01	446.75	1.05
RAP-40 & RCA-60	354.30	0.98	–	–
RAP-20 & RCA-80	396.65	0.98	487.64	0.99

4. CONCLUSIONS

The compressive behavior of LGST columns filled with concrete including RA was investigated experimentally and theoretically in this study. Three types of coarse aggregates

Brought to you by University of Debrecen | Unauthenticated | Downloaded 06/17/22 01:51 PM UTC

were used for the construction the columns with different combinations (RCA & NA, RAP & NA, and RAP & RCA). According to the results, the following conclusions are drawn from this study:

1. Increasing the amount of RCA or RAP aggregates in composite columns decrease the axial compressive capacity. The reduction ratio compared to NA-100 specimens was recorded as 1–14% and 11–18% for 2 and 2.4 mm steel thickness including 40–100% RAP aggregate respectively, and 2–21% and 2–17% for 2 and 2.4 mm steel thickness including 20–100% RCA, respectively.
2. The RAP & RCA composite columns showed a 12–21% reduction in capacities for specimens with 2 mm steel thickness and 13–16% for specimens with 2.4 mm steel thickness, in comparison with the specimen with NA-100.
3. The optimum amount for using RCA or RAP as an alternative to NA has been reported at 20% of replacement. RAP-20 & NA-80 composite specimens recorded approximately the same capacity as the NA-100 composite specimens, while the reduction ratio was recorded as 2% for RCA-20 and NA-80 composite specimens.
4. Composite specimens with RAP gave slightly higher capacities than that for the RCA composite specimens at the same replacement levels. This indicates that the enhancement in the strength of concrete due to confinement is more effective in concrete including RAP than that including RCA, although compressive strength of concrete including RCA is higher than that containing RAP.
5. For concrete only columns, RCA & NA specimens recorded the lowest reduction in capacity compared with results of RAP & NA and RAP & RCA specimens. Capacity Reductions were 20–48%, 12–38%, and 33–41% for specimens including RAP, RCA, and RAP & RCA, respectively.
6. The carrying capacity of light–gauge steel tubes filled with concrete including RCA, RAP, and a combination of RCA and RAP aggregate can be conservatively predicted by AISC and EC4 recommendations, where the EC4 method gives closer predictions of the test results than the AISC method.
7. The existing finite element model proposed in this study can predict the test results of light–gauge steel tubes filled with concrete including RCA, RAP aggregate reasonably well.
8. The LGST columns filled with concrete including RA can be used in small to medium sized buildings with low to medium compressive strength.

ACKNOWLEDGMENTS

The authors would like to gratefully acknowledge the financial support from Deanship of Scientific Research at The University of Jordan.

REFERENCES

[1] W. L. Cortés-Puentesa, D. Palermo, A. Abdulridha, and M Majeeda, "Compressive strength capacity of light gauge steel composite columns," *Case Stud. Constr. Mater.*, vol. 5, pp. 64–78, 2016.

[2] S. De Nardin and A. L. El Debs, "Axial load behavior of concrete-filled steel tubular columns," *Struct. Build.*, vol. 159, no. SB1, pp. 1–10, 2006.

[3] A. K. Patidar, "Behavior of concrete filled rectangular steel tube column," *IOSR J. Mech. Civil Eng.*, vol. 4, no. 2, pp. 46–52, 2012.

[4] L. H. Hana, W. Liub, and Y. F. Yangc, "Behavior of concrete-filled steel tubular stub columns subjected to axially local compression," *J. Constr. Steel Res.*, vol. 64, no. 4, pp. 377–87, 2008.

[5] Y. M. Hunaiti, "Composite action of foamed and lightweight aggregate concrete," *J. Mater. Civil Eng.*, vol. 8, no. 3, pp. 111–3, 1996.

[6] Y. M. Hunaiti, "Strength of composite section with foamed and lightweight aggregate concrete," *J. Mater. Civil Eng.*, vol. 9, no. 2, pp. 58–61, 1997.

[7] M. Etxeberria, E. Vazquez, M. Mari, and M. Barra, "Influence the amount of recycled aggregate and production process on properties of recycled aggregate concrete," *Cement Concrete Res.*, vol. 37, pp. 735–42, 2007.

[8] K. N. Rahal, "Mechanical properties of concrete with recycled coarse aggregate," *Build. Environ.*, vol. 42, no. 1, pp. 407–15, 2007.

[9] R. Larbi, M. Morsli, A. Bali, and E. H. Benyoussef, "Mechanical and elastic properties of concrete made with recycled asphalt pavement," *Int. J. Adv. Mech. Civil Eng.*, vol. 4, no. 3, pp. 1–5, 2017.

[10] F. O. Okafor, "Performance of recycled asphalt pavement as coarse aggregate in concrete," *Leonardo Electron. Practices Tech.*, vol. 17, pp. 47–85, 2010.

[11] N. Shatarat, H. Katkhuda, K. Hyari, and I. Asi, "Effect of using recycled coarse aggregate and recycled asphalt pavement on the properties of pervious concrete," *Struct. Eng. Mech.*, vol. 67, no. 3, pp. 283–90, 2018.

[12] H. Kathuda, N. Shatrat, and K. Hyari, "Effect of silica fume on mechanical properties of concrete containing recycled asphalt pavement," *Struct. Eng. Mech.*, vol. 62, no. 3, pp. 357–64, 2017.

[13] P. Solanki and B. Dash, "Mechanical properties of concrete containing recycled materials," *Adv. Concrete Construction*, vol. 4, no. 3, pp. 207–20, 2016.

[14] Y. F. Yang and L. H. Han, "Compressive and flexural behavior of recycled aggregate concrete filled," *Steel Compos. Struct.*, vol. 6, no. 3, pp. 257–84, 2006.

[15] I. S. Ignjatovic, S. Marinković, Z. Miskovic, and A. Savić, "Flexural behavior of reinforced recycled aggregate concrete beams under short-term loading," *Mater. Structures*, vol. 46, no. 3, pp. 1045–59, 2013.

[16] H. I. Kathhuda and N. Shatarat, "Shear behavior of reinforced concrete beams using treated recycled concrete coarse aggregates," *Construction Building Mater.*, vol. 125, pp. 63–71, 2016.

[17] Y. F Yang and L. H. Han, "Experimental behavior of recycled aggregate concrete filled steel tubular columns," *J. Constr. steel Res.*, vol. 62, no. 12, pp. 1310–24, 2006.

Brought to you by University of Debrecen | Unauthenticated | Downloaded 06/17/22 01:51 PM UTC

[18] N. Shatarat, A. Abed Al-Haq, H. Katkhuda, and M. Abdel Jaber, "Investigation of axial compressive behavior of reinforced concrete columns using recycled coarse aggregate and recycled asphalt pavement aggregate," *Constr. Build. Mater.*, vol. 217, pp. 384–93, 2019.

[19] R. El- Nimri, M. S. Abdel Jaber, Y. M. Hunaiti, and M. Abdel Jaber, "Behavior of light–gauge steel beams filled with recycled concrete," *Mag. Civil Eng.*, vol. 101, no. 1, 2020.

[20] AISC– LRFD, *Load and Resistance Factor Design Specification for Structural Steel Building*. Chicago, U.S.A: American Institute of Steel Construction (AISC), 1999.

[21] Eurocode 4, Design of Composite Steel and Concrete Structures – Part 1-1: General Rules and Rules for Building. European Standards, EN 1994-1-1, 2004.

[22] ASTM, "A370: standard test methods and definitions for mechanical testing of steel products," *ASTM Int.*, pp. 1–50, 2014.

[23] Bulletin A.C.I.E, *Aggregate for Concrete Developed by ACI Committee E-701*. USA, 2007.

[24] AISI, *North American Specification for the Design of Cold-Formed Steel Structural Members*. USA: American Iron and Steel Institute (AISI), 2007.

[25] ACI 318-14, *Building Code Requirements for Structural Concrete and Commentary*. Michigan, USA: American Concrete Institute, 2014.

[26] N. Linh Tran and C. A. Graubner, "Uncertainties of concrete parameters in shear capacity calculation of RC members without shear reinforcement," *Beton-Und Stahlbetonbau Int. Probabilistic Workshop 2018*, vol. 113, no. S2, pp. 1–8, 2018.

[27] R. Allouzi, A. Alkloub, H. Naghawi, and R. Al-Ajarmeh, "Fracture modeling of concrete in plain and reinforced concrete members," *Int. J. Civil Eng.*, vol. 17, no. 7, pp. 1029–42, 2019.

Open Access. This is an open-access article distributed under the terms of the Creative Commons Attribution-NonCommercial 4.0 International License (https://creativecommons.org/licenses/by-nc/4.0/), which permits unrestricted use, distribution, and reproduction in any medium for non-commercial purposes, provided the original author and source are credited, a link to the CC License is provided, and changes – if any – are indicated.

Brought to you by University of Debrecen | Unauthenticated | Downloaded 06/17/22 01:51 PM UTC